Fluids, both ionic and nonionic, over wide ranges of temperature and composition

(Rossini Lecture)

KENNETH S. PITZER

Department of Chemistry and Lawrence Berkeley Laboratory,
University of California, Berkeley, California 94720, U.S.A.

<u>Abstract</u> - After a brief historical review of the determination of
standard state properties of hydrocarbons, the present status of nonideal
gas and liquid state properties is considered. The accuracy to which
various fluids follow the acentric factor system is examined. The shapes
of vapor-liquid and liquid-liquid coexistence curves are considered with
comparisons of theory and experiment for both short-range and long-range
attractive forces. The effective critical exponent β_e is a sensitive
measure of the shapes of these curves. Systems with short-range forces
have low β_e throughout the entire range of temperature and never approach
the high values of mean-field theories. Ionic systems show $\beta_e \simeq 0.5$ over
wide ranges of temperature. The apparent conflict between the theoreti-
cal value 0.325 and a reasonable extrapolation of the experimental β_e to
0.35-0.36 for Ar and Xe at the critical temperature is discussed in
relation to the model used in current theory and the desirability is
expressed for a better model for the vapor-liquid system. An equation of
state is described for NaCl-H_2O which is valid at the critical point of
H_2O and over the coexistence surface to 873 K. Equations are considered
for mixed aqueous electrolytes of unlimited complexity valid for liquid-
like densities. Recent results for Na_2SO_4(aq) to 573 K are described,
together with their use in predictions of solubilities in both Na_2SO_4-H_2O
and in Na_2SO_4-NaCl-NaOH-H_2O.

INTRODUCTION

While I shall give primary attention to recent research, some historical remarks seem
appropriate -- especially since some will concern Dr. Rossini. It was in 1935 that I
started my Ph.D. thesis research with Wendell Latimer at the University of California at
Berkeley. Initially, it concerned the entropies of aqueous ions, and several papers were
published in that area. Before long, the opportunity arose to collaborate with J. D. Kemp
on the problem of restricted internal rotation in ethane and the determination of the
barrier from the entropy and other thermodynamic data. Kemp provided the entropy value; I
provided the quantum statistical mechanics. Soon thereafter, I proceeded from the ethane
problem to those for several other light hydrocarbons. Next came the development of
statistical thermodynamic methods for the prediction of entropies, heat capacities, and
related properties for various series of hydrocarbons with experimental input required for
only one or two initial members. These last capabilities caught the attention of Dr.
Rossini, and he asked me to cooperate or collaborate in assembling tables of thermodynamic
properties for various hydrocarbons. His group measured heats of combustion and obtained
thereby the heats of formation while I provided heat capacities, entropies, and free-energy
functions. This information made possible a more detailed and scientific era for the
petroleum industry. Fred Rossini was at the National Bureau of Standards while I was at
Berkeley except for a period during World War II. The American Petroleum Institute
supported my program as well as Rossini's.

Our collaboration continued for over twenty years, but both Fred and I took up new research
interests in other areas as well as administrative responsibilities. Thus, the hydrocarbon
thermodynamic tables received a diminishing portion of my attention and of his. He arranged
for me to be a member of the IUPAC Commission on Chemical Thermodynamics which he chaired.
After I became President of Rice University, that obligation, together with other
responsibilities, were so demanding that I asked not to be reappointed to the IUPAC
Commission.

My friendship with Fred Rossini continued after our scientific collaboration had ended. He
has been retired now for some time and lives in a retirement community in Florida. I last
saw him at a meeting of the National Academy of Sciences about three years ago, but I wrote
him recently about this Conference. He replied and asked me to extend his greetings to his
many friends at the Conference.

My interest in the statistical thermodynamic calculations related to the information provided about molecular structure as well as to the resulting thermodynamic functions. In addition to internal rotation, other complex molecular motions were identified and studied including pseudorotation in five-membered rings and double-minimum vibrations. Ring strain energies as well as strain energies of ring substituents were studied. Another topic was the bonding in polyatomic carbon molecules and their thermodynamics.

In 1971 I concluded my major administrative responsibilities and shifted my primary attention back to science including both molecular structure and thermodynamics. Recent topics with both structural and thermodynamic aspects include the multidimensional pseudorotation in XeF_6 (ref. 1) and the very interesting properties of solid CH_4 near 1 K where heat capacity measurements showed a sharp peak (ref. 2). Another area was the relativistic quantum theory for molecules containing very heavy atoms (ref. 3). In one example, an apparent anomaly in the experimental dissociation energy of Pb_2 was resolved.

FLUID STATE

Most of the topics considered so far relate to the thermodynamic properties in the ideal gas state. But many important systems are liquids or dense and very nonideal gases. Thus, I began very early to take some interest in the fluid state over its full range of density. With the advance of quantum mechanics, it became possible to identify groups of molecules that should follow corresponding states principles in their fluid behavior (refs. 4,5). The simplest such group comprises argon, krypton, xenon, and methane which I called simple fluids (ref. 6), and to which I shall return.

Out of this work grew extensions of corresponding states with additional parameters. My proposal in this area was the acentric factor system which was and is widely used (refs. 6,7). The acentric factor relates to the increase in slope of the vapor-pressure curve as compared to simple fluids for which the factor is defined as zero. This quantity is accurately measurable from readily available data. Then various properties are given as functions of the critical temperature and pressure and the acentric factor.

Dr. Schreiber and I recently revisited this area and proposed improved working equations within the original definition (ref. 8). With recent experimental investigations of high precision, it is possible to examine the accuracy to which real fluids follow the acentric factor system. Figure 1a shows the deviations between measured and calculated pressures for the simple fluids along the critical isotherm and at a higher temperature. The agreement is essentially perfect up to a reduced density of about 1.5, after which considerable deviations arise at $T_r = 1$. In this relatively incompressible region, a more realistic criterion is the deviation in density at a given pressure. On this basis, the deviations are lower by a factor of 5 to 10 but are still well outside of experimental uncertainty.

On a structural basis, corresponding states require complete similarity of intermolecular potentials with energy and distance scaling factors specific to each substance. Apparently the outer portions of the curves for argon, krypton, xenon and methane fulfill this requirement quite accurately, but there are differences in the shape of the inner or repulsive region that become important at high densities. It is interesting that the polyatomic methane falls close to krypton and between argon and xenon. Thus, the deviation of methane from spherical shape is not important for the intermolecular potential. Figures 1b,c,d show some other comparisons for various fluids with our new equation of state in the acentric factor system. It is clear that the acentric factor system gives very accurate predictions to a reduced density of about 1.5 and useful but less precise estimates at higher densities.

The calculation of fluid properties from intermolecular potentials is difficult and most results, even today, relate to simplified models or to the second virial coefficient. Nevertheless, it is important to keep the structural aspect in mind, and I shall now make some historical remarks in that respect.

Liquids are sometimes pictured as irregular arrays of molecules and vacancies, holes of molecular size. A connection is then made to order-disorder theories for lattices. For many purposes, I believe that the difference between a symmetrical or an irregular lattice is unimportant. Thus, for mixing in a liquid of molecules of similar sizes, the lattice order-disorder model is very useful.

But for pure fluids and their vapor-liquid relationship, the question concerns the molecular-sized holes. Some rather successful calculations have been based on the hole picture. But computer simulations by Monte Carlo or molecular dynamics methods gave a rather detailed picture of the structure of simple fluids of varying density and did not support the hole model. The vacant spaces have various shapes and sizes and are not primarily holes of molecular size.
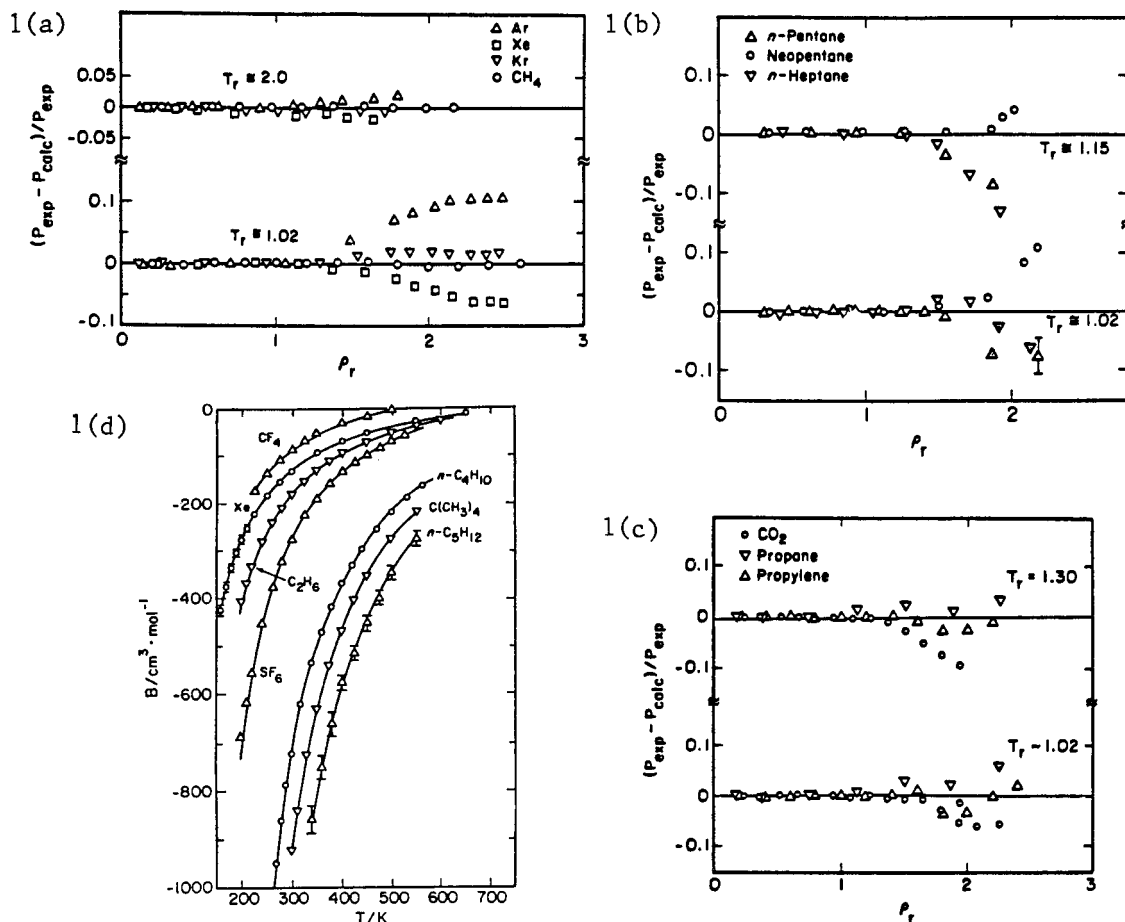
Fig. 1. Deviations of experimental pressures from the acentric factor equation (a,b,c); Comparison of calculated and experimental second virial coefficients (d).

Thus, the hole theory for expanded liquids has largely been abandoned except for one application. It is still used for the near-critical properties. The reference here is to disorder or spin reorientation on a lattice (the Ising lattice model). Then the "universality principle" is interpreted to indicate that vapor-liquid properties follow this same pattern. The experimental evidence from measurements extremely close to the critical point is consistent with this interpretation. But the behavior less close to critical is different for vapor-liquid systems than for lattice or for liquid-liquid systems, as I shall show presently.

Before returning to the near critical region, I shall examine the shapes of vapor-liquid and liquid-liquid coexistence curves well away from the critical point (see refs. 8 and 9 for additional details). Figure 2a shows the shape of this curve for argon. The curve is almost exactly cubic, i.e.,

$$(\rho_1 - \rho_v)^3 = (\text{const.})(1-T_r) \tag{1}$$

with ρ_1 and ρ_v the liquid and vapor densities, respectively, and T_r the reduced temperature.

But no simple equation of state yields a cubic coexistence curve. Any mathematically analytical equation gives a parabolic (2nd power) curve close to the critical point. Various theories for fluids, from van der Waals on, contain approximations which are often called "mean field approximations" and which replace the real forces by long-range forces. And it has been shown rigorously that, for long-range interparticle forces, the parabolic curve is correct over a wide temperature range. But for argon and most real fluids the curve is cubic. This confusing situation can now be clarified by two types of recent results.

First is the recent theoretical calculation for the 6-12 or Lennard-Jones (L-J) potential by Monte Carlo methods in the Gibbs ensemble by Panagiotopoulos (ref. 10). The resulting vapor-liquid curve is closely cubic and agrees very well with that for argon as shown on Fig. 2a. This shows that the parabolic, mean-field curves are never correct even far from the critical point.
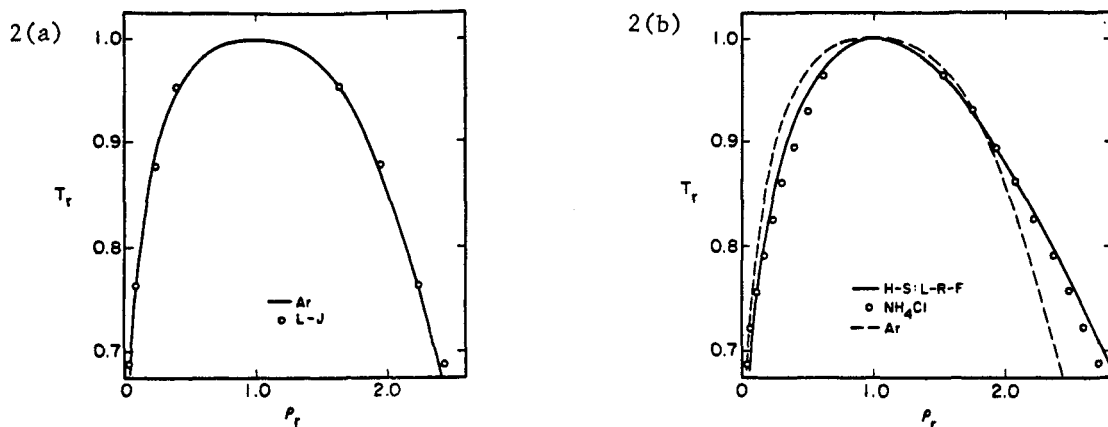
Fig. 2. Coexistence curves; (a) for argon and the Lennard-Jones model; (b) for NH_4Cl, Ar, and the hard-sphere; long-range-force (HS:LRF) model.

It is sometimes suggested that the cubic character of the coexistence curve is related to the long-range fluctuations near the critical point. We now know that this is not correct. The Monte Carlo calculations involved 500 molecules and could not include long-range fluctuations, yet they yield a cubic curve. Thus, this cubic character over most of the temperature range has no connection to near-critical fluctuation effects.

The second type of recent information comes from the real systems with relatively long-range forces, ionic systems. There is, as yet, no good theory for the near-critical behavior of an ionic fluid, but there are experimental data from Buback and Franck (ref. 11) for NH_4Cl. Its coexistence curve is parabolic and is close to that calculated for a fluid with hard-sphere repulsion and infinitely long-range force of attraction (H-S:L-R-F). Figure 2b shows that curve, the NH_4Cl data, and the argon curve for comparison. $T_c = 1155$ K for NH_4Cl.

Very recently, my colleagues and I have found two ionic, liquid-liquid systems that model a pure ionic fluid. Both give accurately parabolic curves

$$(x'' - x')^2 = (\text{const.})(1-T_r) \tag{2}$$

where x'' and x' are the respective mole fractions. The systems are tetra-n-butylammonium picrate: 1-chloroheptane (ref. 12), with $T = 414.4K$ and n-butyl triethylammonium n-butyl triethylboride: diphenyl ether (ref. 13) with $T_c = 316.7K$. In each case the ions have only very nonspecific interparticle forces in addition to the coulomb forces, but their large size makes it possible to obtain criticality at a low temperature where detailed measurements are feasible.

My lecture two years ago at Lisbon (ref. 14) comprised a general discussion of ionic fluids and included other pertinent aspects which will not be repeated here. But some of these reinforce the conclusion that there is a general difference between the properties of ionic and nonionic fluids. We now add that, for the shape of the coexistence curve, the ionic fluids follow the pattern calculated for fluids with infinitely long-range attractive forces.

CRITICAL EXPONENTS

A sensitive method for describing near-critical behavior is the use of critical exponents. These are usually defined in the limit as the critical point is approached. But it is also useful to consider effective exponents valid at a distance from the critical point. We consider the effective β_e for the coexistence curve defined as

$$\beta_e = \Delta\ln(\rho_1 - \rho_v)/\Delta\ln(1-T_r) \tag{3}$$

This quantity was first defined by Verschaffelt in 1896 (ref. 15). He discovered many important aspects of coexistence curves including their cubic nature which were, however, ignored and rediscovered later. Dr. Levelt Sengers has written an interesting history of this period (ref. 16).

Figure 3a shows the effective β_e for argon and xenon together with values calculated for the L-J model. It is evident that they agree well within the statistical uncertainties of the calculations. Also shown are curves for H_2O, for the hard-sphere, long-range-force (H-S:L-R-F) model, and for the Ising lattice (simple cubic). For the vapor-liquid systems with short-range forces, the curves naturally extrapolate to about 0.36 at the critical point, whereas the currently accepted theory predicts that the critical value should be that of the
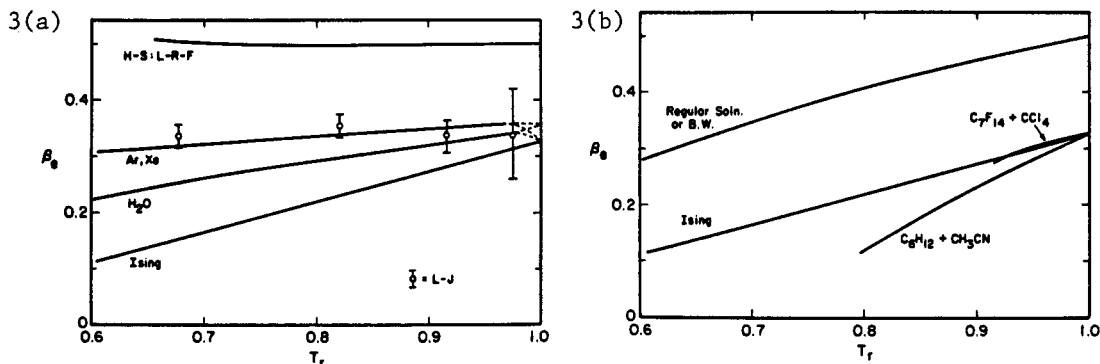
Fig. 3. Effective β_e: (a) for Ar, Xe, H_2O and three model systems; (b) for two models and two experimental liquid-liquid systems.

Ising lattice, 0.325. There is experimental evidence consistent with the 0.325 value for the limiting β; this implies that the effective β_e curves downward in the range 0.98 - 1.00 in T_r as shown by the lower dashed curves. In contrast, there is no change in slope of the Ising curve in this region; it is positive and nearly constant throughout the entire range.

Figure 3b shows the effective β_e for two nonionic liquid-liquid systems with short-range forces. Both have curves similar to the Ising curve and extrapolate naturally to the value 0.325 at the limit. Also shown is the curve for the mean-field model appropriate for liquid-liquid mixing (Regular Solutions or Bragg-Williams); one notes that it has a positive slope in contrast to the nearly constant β_e for the vapor-liquid case.

From Figures 3a and b, it is very clear that one-component, vapor-liquid coexistence curves are distinctly different from those of two-component, liquid-liquid systems as they approach the critical temperature. Assuming the correctness of the Ising limit for the vapor-liquid systems, the difference is the sudden shift from positive to negative slope near $T_r = 0.98$. It would be most desirable to have a good theory for near-critical, vapor-liquid behavior for short-range forces. Such a theory could confirm the qualitative aspects of the lower dashed curves on Figure 3a.

The possibility that the limiting exponent for the vapor-liquid system differs from the Ising value should also be kept in mind. Rowlinson and Swinton (ref. 17) regard this to be an open question. In his original proposal of the principle of universality, Kadanoff (ref. 18) states the criteria as: dimensionality, symmetry of the order parameter, and perhaps other criteria. This difference between the vapor-liquid situation and the spin lattice would be "another criterion." Also, Baker (ref. 19) has presented examples in other universality classes where critical exponents are shown to depend on such additional criteria.

Recent papers (refs. 20,21) show that near-critical experimental data are consistent with the Ising limit, but the authors assume that limit and introduce numerous correcting terms which are adjusted. These papers were written, in part, to refute an earlier assertion of Garland and Thoen (ref. 22) that their data "are incompatible with the Ising β." I discussed this situation with Dr. Garland, and he now agrees that his and other data can be fitted to the Ising β. But I have seen no definitive proof that the experimental data for vapor-liquid systems cannot be fitted to a higher β in the range 0.34 - 0.36. Indeed the Garland-Thoen paper indicates that this is possible. Again, I say that our greatest need is a good theory for a vapor-liquid system in the critical region, a theory that does not imply that the vacant space is in holes of molecular size.

Regardless of the limiting β, it is clear that the effective β_e for nonionic vapor-liquid systems does not approach mean-field behavior at lower temperature. Thus, treatments comprising a near-critical equation and a "crossover" should use a far-field equation with the correct effective β_e and not one with $\beta_e = 0.5$. The original crossover treatment of Chapela and Rowlinson (ref. 23) satisfies this requirement, but some subsequent treatments do not.

A final conclusion to be drawn from Figures 2b and 3a concerns the difference between fluids with long-range forces and those with short-range forces. The difference in β_e extends over the entire range of temperature. If this difference were limited to long-range fluctuations, it would disappear as the temperature decreases from critical. The fact that the difference does not disappear means that it involves local distributions and motions. Forces of infinite range have no effect on local motions while short-range forces do have an effect; thus there is a clear case for a difference. The difference for the ionic case is more complex. The attraction of unlike charges and the repulsion of like charges has a major effect on the local structure. The structural influence of these forces will decrease with increase in temperature. I have considered some of these aspects of ionic fluids elsewhere (refs. 24,25).

THE SYSTEM NaCl–H₂O NEAR THE CRITICAL POINT OF WATER

Near critical water with sodium chloride impurity is of major importance in steam power engineering, while the same system with large or small concentrations NaCl is important geologically.   I had dealt with this system by several methods appropriate to conditions away from the critical point of water.   At Lisbon I described the model for NaCl in steam based on successive hydration equilibria (refs. 14,26).   Other methods dealt with liquid-like solutions well below the critical point of water (ref. 27) and a hydrated, fused-salt model valid for high concentrations at any temperature above 400 K (ref. 28).

There are special complexities for a two-component system close to the critical point of one component which were avoided in these treatments.   John Tanger and I have now found a relatively simple equation which works remarkably well near the critical point of water (647 K) and along the NaCl-H₂O critical line up to 873 K (ref. 29).   With somewhat reduced accuracy it fits the entire phase coexistence surface from 523 to 873 K.

The basis is a simple perturbation by the NaCl of the equation of state for H_2O.   The initial assumption for the fluid pressure is the series

$$P = P_{H_2O}(T,d) + y[b_{10}+b_{11}(d-1) + ...] + y^2[b_{20} + ...] + ...\qquad(4)$$

where d is the reduced density of water in the system, $[\rho(H_2O)/\rho_c(H_2O)]$ with $\rho_c(H_2O)$ the critical density of pure water, and y is the mole ratio n_{NaCl}/n_{H_2O}.   Although additional terms could easily have been included, the three shown sufficed.[2]   The initial term is just the pressure of pure water at the water-density and temperature of the system (ref. 30). b_{10} gives the linear effect of NaCl on that pressure at critical density while b_{11} gives the change in that effect with water-density.   The final term is small except at high NaCl concentrations and represents NaCl-NaCl interactions.   Each of these parameters is temperature dependent.
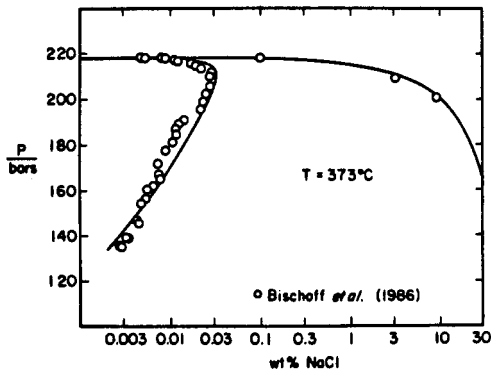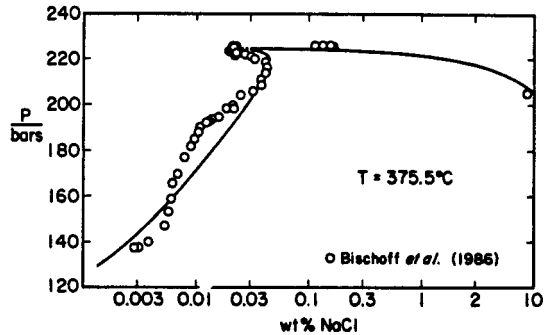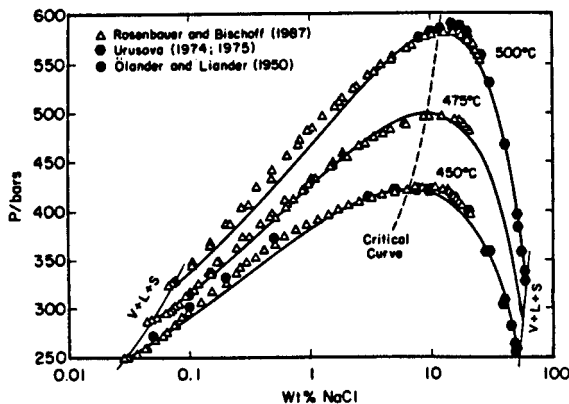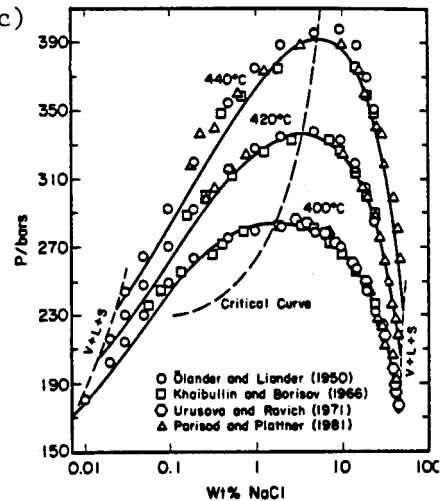

Fig. 4.   The coexistence curve for NaCl-H₂O: (a) at 373.0°C (646.2 K); (b) at 375.5°C (648.7 K); (c), (d) at several temperatures.

The Helmholtz energy is obtained by integration with pressure and the addition of pressure-independent terms: one for ideal mixing and another proportional to the NaCl content. The molar Gibbs energy then takes the simple form

$$G/(n_{H_2O} + n_{NaCl}) = (1-x)g_{H_2O}(T,d) + xv_c b_{11}(1+lnd)$$
$$+ RT[xlnx + (1-x)ln(1-x)] + xg_{NaCl}^*(T) \qquad (5)$$

Now x is the mole fraction y/(1+y) and v_c is the critical volume of water. The coexisting compositions can now be obtained by first calculating the density as a function of x (or y) at constant T and P from equation (4) (by iteration). Equation (5) then gives the molar Gibbs energy as a function of mole fraction and the common tangent locates the compositions at equilibrium.

By trial and adjustment the parameters were first obtained for several temperatures, then the temperature-dependent expressions were developed, and the results tested by recalculation of the coexistence surface. Figures 4a-d show comparisons of calculated curves with phase equilibrium data (refs. 31-36).

Since the g* term is linear in x, it does not affect the coexistence surface. But it can be obtained from the chemical potential of NaCl given by

$$\mu_{NaCl} = RTlnx + v_c[-b_{10}/d + b_{11}(lnd + 1/d)] - 2v_c yb_{20}/d + g_{NaCl}^*(T) \qquad (6)$$

This equation can be applied along the three-phase line for equilibrium with solid NaCl or at any other point where the chemical potential of NaCl is known.

Appropriate derivatives of the Helmholtz energy give various thermodynamic properties. Examples are

$$(\partial P/\partial T)_d = (\partial P_{H_2O}/\partial T)_d + y[(db_{10}/dT) + (d-1)(db_{11}/dT)] + y^2(db_{20}/dT) \qquad (7)$$

$$(dP/\partial d)_T = (\partial P_{H_2O}/\partial d)_T + yb_{11} \qquad (8)$$

$$C_v/n_{H_2O} = c_{v,H_2O}(T,d) + yv_c(T/d)[(d^2b_{10}/dT^2) + y(d^2b_{20}/dT^2)$$
$$- (dlnd+1)(d^2b_{11}/dT^2)] + y\, c_{NaCl}^*(T) \qquad (9)$$

where $c_{NaCl}^*(T)$ is the appropriate derivative of $g_{NaCl}^*(T)$. These quantities can be combined to yield the heat capacity at constant pressure. Comparison with experimental data at liquid-like density indicated that c* was negligible at high temperature and that the lower-temperature behavior was represented by

$$c_{NaCl}^*/R = -2.36 \times 10^{46} T^{-16} \qquad (10)$$

We then calculated the apparent molar heat capacity for comparison with the measurements of White et al. (ref. 37) along a near-critical path (321 bars, 32.1 MPa) from 600 to 700 K. Figure 5 shows the remarkable agreement with all of the striking features in this range. If our curve were shifted downward in temperature by a few degrees, the agreement would be nearly perfect.

The resulting equations for various temperature-dependent parameters are

$$b_{10} = -29984.4 + 19.0285T + 6.65541 \times 10^{12}/T^3 - 1.20069 \times 10^{18}/T^5 \qquad (11)$$

$$b_{11} = 3928.3 - 10.5947T - 6.0751 \times 10^{38}/T^{13} \qquad (12)$$

$$b_{20} = 14121.9 - 27.0731T - 2.57142 \times 10^{23}/T^7 \qquad (13)$$

$$[g_{NaCl}^*(T) - H_{298}^{\circ}]/RT = 1.0 \times 10^{44} T^{-16} + 1900/T - 10.0 \qquad (14)$$

where the reference state H_{298}° is for solid NaCl and the units are bars for b_{10}, b_{11}, b_{20}.

Comparisons were made with various other measured quantities including densities and enthalpies, which had not been used in parameter evaluation. The agreement is very good for near-critical compositions or for total fluid properties at low densities. Moderate discrepancies appear for very high concentrations or for partial molar properties of the NaCl at low densities.
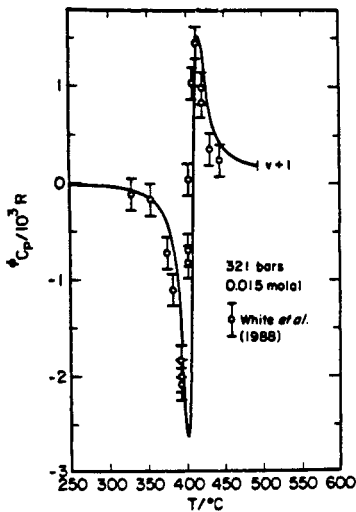
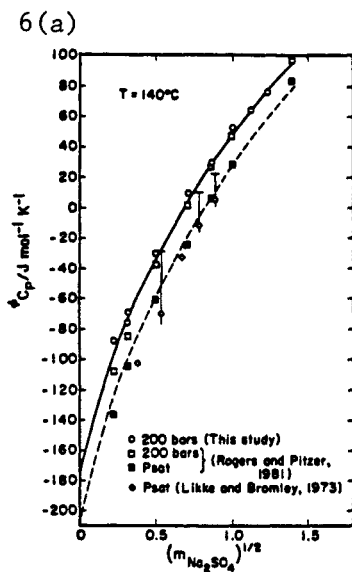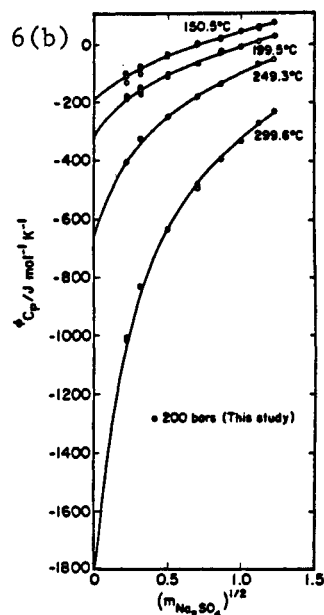**Fig. 5.** Apparent molar heat capacity of NaCl in H_2O.

Fig. 6a,b. Apparent molar heat capacity of Na_2SO_4 in H_2O.

ACTIVITY COEFFICIENTS AND SALT SOLUBILITIES IN AQUEOUS SOLUTIONS AT HIGH TEMPERATURES

At more moderate temperatures, aqueous salt solutions can be treated by the same equations that have been successful at room temperature. I discussed this subject at the Second IUPAC Symposium on Solubility Phenomena in greater detail than is possible here (ref. 38). But I do want to report certain very recent results, as an example of the methods, the measurements, and typical applications.

The fundamental theoretical approach is a virial expansion within the McMillan-Mayer framework. But this must be modified to handle electrostatic forces following Mayer and particularly Friedman (ref. 39). Also, I converted from the Helmholtz energy basis, with variables concentration and temperature, to the Gibbs energy basis with variables molality and temperature. Finally, term rearrangements are required since electrical neutrality must be maintained. The excess Gibbs energy per kg of water for an indefinitely complex mixture can then be expressed as

$$G^{ex}/(w_w RT) = f(I) + 2 \sum_c \sum_a m_c m_a [B_{ca}(I) + (\sum_c m_c z_c) C_{ca}]$$

$$+ \sum_{c<c'} \sum m_c m_{c'} [2\Phi_{cc'}(I) + \sum_a m_a \psi_{cc'a}] + \sum_{a<a'} \sum m_a m_{a'} [2\Phi_{aa'}(I) + \sum_c m_c \psi_{caa'}]$$

$$+ 2 \sum_n \sum_c m_n m_c \lambda_{nc} + 2 \sum_n \sum_a m_n m_a \lambda_{na} + 2 \sum_{n<n'} \sum m_n m_{n'} \lambda_{nn'} \qquad (15)$$

Here the dependency of certain quantities on ionic strength is indicated, f(I) includes the Debye-Huckel limiting law but is an extended form, while c, a, n represent cation, anion, and neutral solute species, respectively. The B_{ca}'s and C_{ca}'s are second and third virial coefficients, or binary and ternary interaction parameters, specific to the c-a interaction and can be determined from the pure c-a electrolyte. The Φ_{ij} and ψ_{ijk} are parameters for the difference of interaction of unlike ions of the same sign from the mean of like ions, and can be measured from common-ion mixtures such as $NaCl-KCl-H_2O$ or $NaCl-NaNO_2-H_2O$. The last three sums add the binary iterations involving neutral species with ions and with one another. The osmotic coefficient and the various activity coefficients are given by appropriate derivatives of G^{ex} in terms of the same parameters. Further details are given in any of several reviews (refs. 38,40-42).
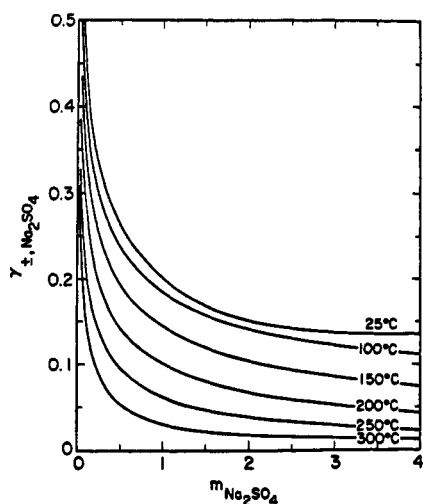
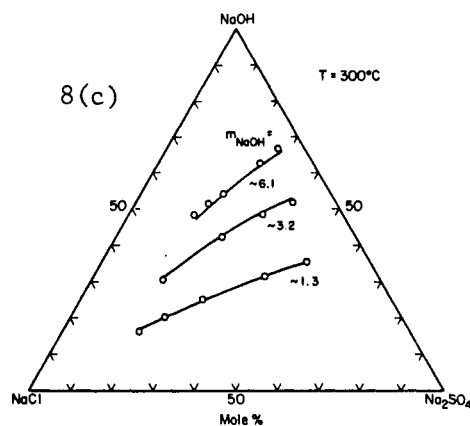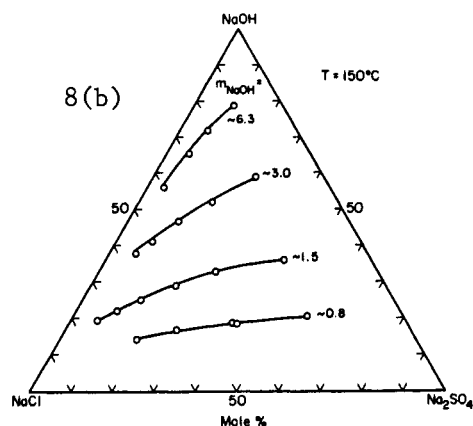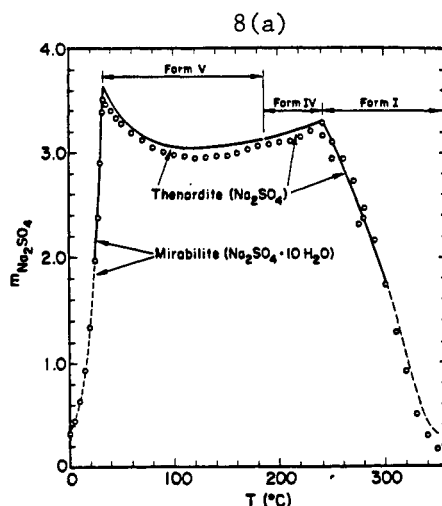**Fig. 7.** Activity coefficient of Na$_2$SO$_4$(aq) at various temperatures.

Fig. 8. Comparison of predicted and measured solubilities of Na$_2$SO$_4$ in water (a) and in solutions with NaOH and NaCl (b,c).

In addition to the excess quantities, one needs the standard-state properties as a function of temperature and pressure. If these are known at 298.15 K, heat capacity measurements allow the calculation of the standard-state properties at higher temperature. And measurements at different molalities allow integration of the excess properties to higher temperatures. Thus, we have been measuring the heat capacities of the solutions of important salts. I present results currently in press for Na$_2$SO$_4$ as an example (ref. 43). Figure 6a compares the new measurements at 140°C with previous measurements (refs. 44,45) and shows the change with pressure, while Fig. 6b shows the new results for higher temperatures.

These heat capacities were combined with all other data, mostly for 298 K, to yield a complete equation for aqueous Na$_2$SO$_4$ valid to 573 K. Figure 7 shows the resulting activity coefficients. Figure 8a compares the predicted solubility of the different crystalline forms of Na$_2$SO$_4$ with experimental values. The agreement is remarkably good even in extrapolation above 300°C. Finally, this equation for Na$_2$SO$_4$ was combined with comparable equations for NaCl and NaOH and with the mixing parameters determined from common ion NaCl-Na$_2$SO$_4$, NaCl-NaOH, and NaOH-Na$_2$SO$_4$ mixtures to predict solubilities in the quaternary system Na$_2$SO$_4$-NaCl-NaOH-H$_2$O (Fig. 8b,c, ref. 46).

It is the capacity to predict properties in multicomponent mixtures that I want to emphasize. Natural brines and many industrial fluids have many components, and the individual measurement of each composition would be enormously expensive. We now have a reliable method of prediction based on a limited number of parameters measured from single solute and simple binary mixed solute systems. This method is finding more extensive application as its predictive reliability is demonstrated and the data base is extended.

Acknowledgements

REFERENCES

1.   K. S. Pitzer and L. S. Bernstein, J. Chem. Phys. 63, 3849-3856 (1975).
2.   G. J. Vogt and K. S. Pitzer, J. Chem. Thermodyn., 8, 1011-1031 (1976).
3.   K. S. Pitzer, J. Chem. Phys., 74, 3078-3079 (1981); Int. J. Quant. Chem., 25, 131-148 (1984).
4.   J. de Boer and A. Michels, Physica 5, 945-957 (1938).
5.   K. S. Pitzer, J. Chem. Phys. 7, 583-590 (1939).
6.   K. S. Pitzer, J. Am. Chem. Soc. 77, 3427-3433 (1955).
7.   K. S. Pitzer and L. Brewer, Thermodynamics, revision of 1st ed. by G. N. Lewis and M. Randall, Appendix I, McGraw-Hill, New York (1961).
8.   D. R. Schreiber and K. S. Pitzer, Fluid Phase Equilibria, submitted.
9.   K. S. Pitzer, Thermochimica Acta, in press.
10.   A. Z. Panagiotopoulos, Mol. Phys. 61, 813-826 (1987).
11.   M. Buback and E. U. Franck, Ber. Bunsenges. Phys. Chem. 76, 350-354 (1972); 77, 1074-1079 (1973).
12.   K. S. Pitzer, M. C. P. de Lima, and D. R. Schreiber, J. Phys. Chem. 89, 1854-1855 (1985).
13.   R. R. Singh and K. S. Pitzer, J. Am. Chem. Soc., submitted.
14.   K. S. Pitzer, Pure and Appl. Chem. 59, 1-6 (1987).
15.   J. E. Verschaffelt, Commun. Phys. Lab., Leiden, 28, 1-15 (1896).
16.   J. M. H. Levelt Sengers, Physica, 82A, 319-351 (1976).
17.   J. S. Rowlinson and F. L.Swinton, Liquids and Liquid Mixtures, 3rd edition, pp. 82-83, Butterworth Scientific, London (1982).
18.   L. P. Kadanoff, Scaling, Universality and Operator Algebras, in Phase Transitions and Critical Phenomena, C. Domb and M. S. Green, eds, v. 5a, Acad. Press, London (1976).
19.   G. A. Baker, Jr., Phys. Rev. Lett. 60, 1844-1847 (1988) and earlier papers there cited.
20.   H. Guttinger and D. S. Cannell, Phys. Rev. A24, 3188-3201 (1981).
21.   D. Balzasini and O. G. Mouritsen, Phys. Rev. A28, 3515-3519 (1983).
22.   C. W. Garland and J. Thoen, Phys. Rev., A13, 1601-1604 (1976).
23.   G. A. Chapela and J. S. Rowlinson, J. Chem. Soc. Faraday Trans. I 70, 584-593 (1974).
24.   K. S. Pitzer, J. Phys. Chem. 88, 2689-2697 (1984).
25.   K. S. Pitzer and D. R. Schreiber, Mol. Phys., 60, 1067-1078 (1987).
26.   K. S. Pitzer and R. T. Pabalan, Geochim. Cosmochim. Acta, 50, 1445-1454 (1986).
27.   K. S. Pitzer, J. C. Peiper, and R. H. Busey, J. Phys. Chem. Ref. Data 13, 1-102 (1984).
28.   K. S. Pitzer and Yi-gui Li, Proc. Nat. Acad. Sci. USA 81, 1268-1271 (1984).
29.   K. S. Pitzer and J. C. Tanger IV, Int. J. Thermophys., in press.
30.   L. Haar, J. S. Gallagher, and G. Kell, NBS/NRC Steam Tables, Hemisphere, Washington (1984).
31.   A. Olander and H. Liander, Acta Chem. Scand. 4, 1437-1445 (1950).
32.   Kh. Khaibullin and N. M. Borisov, Taplofiz. Vzsok. Temp. 4, 518-523 (1966) (English translation 489-494).
33.   M. A. Urusova and M. I. Ravich, Russian J. Inorg Chem. 16, 1534-1535 (1971).
34.   C. J. Parisod and E. Plattner, J. Chem. Eng. Data, 26, 16-20 (1981).
35.   J. L. Bischoff, R. J.Rosenbauer and K. S. Pitzer, Geochim. Cosmochim. Acta, 50, 1437-1444 (1986).
36.   R. J. Rosenbauer and J. L. Bischoff, Geochim. Cosmochim. Acta 51, 2349-2354 (1987).
36a.   M. A. Urusova, Russian J. Inorg. Chem., 19, 450-454 (1974); 20, 1717-1721 (1975).
37.   D. E. White, R. H. Wood, and D. R. Biggerstaff, J. Chem. Thermo. 20, 159-168 (1988).
38.   K. S. Pitzer, Pure and Appl. Chem., 58, 1599-1610 (1986).
39.   H. L. Friedman, Ionic Solution Theory, Interscience, New York (1962).
40.   K. S. Pitzer, Theory: Ion Interaction Approach, in Activity Coefficients in Electrolyte Solutions, R. Pytkowicz, ed., pp. 157-208, CRC Press, Boca Raton, Florida (1979).
41.   K. S. Pitzer, Rev. Mineralogy, 17, 97-142 (1987).
42.   C. E. Harvie, N. Møller, and J. H. Weare, Geochim. Cosmochim. Acta, 48, 723-751 (1984).
43.   R. T. Pabalan and K. S. Pitzer, Geochim. Cosmochim. Acta, in press.
44.   S. Likke and L. Bromley, J. Chem. Eng. Data, 18, 189-195 (1973).
45.   P. S. Z. Rogers and K. S. Pitzer, J. Phys. Chem., 85, 2886-2895 (1981).
46.   W. C. Schroeder, A. Gabriel, and E. P. Partridge, J. Am. Chem. Soc., 57, 1539-1546 (1935).